Correlation Between Foveal Cone Outer Segment Tips Line and Visual Recovery After Epiretinal Membrane Surgery

Yuji Itoh, Makoto Inoue, Tosho Rii, Kazunari Hirota, and Akito Hirakata

Kyorin Eye Center, Kyorin University School of Medicine, Tokyo, Japan

Correspondence: Makoto Inoue, Kyorin Eye Center, Kyorin University School of Medicine, 6-20-2 Shinkawa, Mitaka, Tokyo, 181-8611, Japan; inoue@eye-center.org.

Submitted: June 29, 2013
Accepted: September 22, 2013

Citation: Itoh Y, Inoue M, Rii T, Hirota K, Hirakata A. Correlation between foveal cone outer segment tips line and visual recovery after epiretinal membrane surgery. *Invest Ophthalmol Vis Sci.* 2013;54:7302–7308. DOI:10.1167/iovs.13-12702

Purpose. To determine whether there is a significant correlation between the integrity of the foveal microstructures and the best-corrected visual acuity (BCVA) after pars plana vitrectomy for epiretinal membrane (ERM) removal.

Methods. This was a retrospective, interventional case series. Forty-six eyes of 45 patients with an ERM underwent vitrectomy. The foveal area was examined by spectral-domain–optical coherence tomography (SD-OCT) preoperatively and postoperatively. The correlation between the length of the photoreceptor cone outer segment tips (COST) line defect, the inner segment/outer segment junction (IS/OS) line defect, the external limiting membrane (ELM) line defect, and the BCVA was determined.

Results. The length of the COST line defect was significantly correlated with the BCVA at postoperative 1, 3, 6, 9, and 12 months ($P < 0.001$ for all). Forward stepwise regression analyses showed that the postoperative BCVA was significantly correlated with the length of COST line defect ($P < 0.001$) but not with the IS/OS line and ELM line defects for up to 6 months. The preoperative length of the COST line defect was significantly correlated with the postoperative BCVA at 12 months ($P = 0.005$), but the lengths of the IS/OS line defect and ELM line defect were not. The factor that best predicted the postoperative BCVA was the length of the preoperative COST line defect ($P = 0.04$) but not the preoperative BCVA ($P = 0.69$).

Conclusions. The recovery of the foveal COST line defect is correlated with the BCVA after ERM surgery. The length of the preoperative COST line defect can predict the potential foveal function. (ClinicalTrials.gov number, NCT01549249.)

Keywords: spectral-domain optical coherence tomography, idiopathic epiretinal membrane, cone outer segment tips, inner segment/outer segment junction, pars plana vitrectomy

An idiopathic epiretinal membrane (ERM) is a relatively common retinal disorder that can be diagnosed and monitored by optical coherence tomography (OCT).[1–3] An ERM causes morphologic alterations of the retina that lead to functional changes such as a decrease of the best-corrected visual acuity (BCVA) and metamorphopsia.[4,5] The surgical removal of an ERM was first reported by Machemer,[6] who showed that the removal restored good BCVA, although the degree of recovery varied.

Spectral-domain–optical coherence tomographic (SD-OCT) instruments allow clinicians to obtain more precise cross-sectional images of the photoreceptors than the earlier OCT instruments.[7–9] Earlier SD-OCT studies showed that an ERM can be associated with structural changes of the foveal photoreceptors, including a disruption of the inner/outer segment junction (IS/OS) line.[2,3,10–13] A preoperative intact IS/OS line was significantly correlated with the postoperative BCVA, and the authors suggested that the integrity of the IS/OS line might be used as a prognostic factor for the postoperative BCVA after ERM removal.[5,11,14–16]

The cone outer segment tips (COST) line is a highly reflective line observed between the IS/OS line and retinal pigment epithelium (RPE) and can be detected in the images obtained by high-speed, ultrahigh-resolution OCT instruments.[17] We have reported that the COST line can also be observed in the images obtained by commercially available SD-OCT in 95% of normal subjects with good BCVA.[18] A disruption of the COST line has been detected in eyes with macular diseases and might be an early sign of photoreceptor disorder.[4,19–23] We have also reported that there was a significant correlation between the postoperative BCVA and the recovery of the foveal COST line after successful macular hole surgery.[24,25] We found that better integrity of the COST line and shorter length of the COST line defect at the fovea were both significantly correlated with better postoperative BCVA after successful macular hole closure. However, whether this significant correlation was specific for eyes after closure of a macular hole or was generally true for eyes with other types of macular diseases such as an ERM has not been determined.

Thus, the purpose of this study was to determine whether the length of the postoperative COST line defect was significantly correlated with the BCVA before and after successful ERM surgery. In addition, we determined the preoperative factors that were significantly correlated with the postoperative BCVA.

Patients and Methods

Of the original 283 eyes, 72 eyes with a secondary ERM, including 23 eyes with history of uveitis, 36 eyes with retinal

Table 1. Patient Baseline Characteristics

No. of eyes (patients)	46 (45)
Age, y, mean ± SD (range)	67.4 ± 7.5 (48–84)
Sex, no. (%)	
Men	19 (43%)
Women	26 (57%)
Eye, no. (%)	
Right	22 (48%)
Left	24 (52%)
Axial length, mm, mean ± SD	23.8 ± 1.1
Preoperative BCVA, logMAR mean ± SD	0.28 ± 0.21
Symptom duration, mo, mean ± SD (range)	15.9 ± 19.2 (1–100)
Preoperative central foveal thickness, μm, mean ± SD	463.0 ± 132.6
Combination of cataract surgery, no. (%)	40 (87%)

SD, standard deviation.

tears, 6 eyes with diabetic retinopathy, 4 eyes with retinal vein occlusion, and 3 eyes with macroaneurysm, were excluded. Eyes with coexistence of asteroid hyalosis, familial exudative vitreoretinopathy, retinal schisis, pigmentary degeneration, and severe cataract (>3 Emery-Little classification) were also excluded. Fourteen eyes with high myopia with an axial length > 27.0 mm or refractive error greater than −8.0 diopters (D), 9 eyes with a pseudomacular hole, and 7 eyes with vitreomacular traction syndrome were excluded. Twenty-two eyes with history of vitreoretinal surgeries and 5 eyes with postoperative complications including retinal detachments were excluded. After exclusion of these 133 eyes, only those with more than 6 months of postoperative follow-up were included. In the end, 46 eyes of 45 patients (19 men, 26 women) met the study criteria for the data analyses.

All patients were diagnosed with an ERM by SD-OCT and had undergone surgery between November 2008 and September 2010 at the Kyorin Eye Center. The preoperative data analyzed were age, sex, right or left eye, axial length, symptom duration, BCVA measured with Landolt C chart, central foveal thickness (CFT), length of the COST line defect, and length of the IS/OS and external limiting membrane (ELM) line defects.

All surgeries were performed after the patients received a detailed explanation of the surgical and SD-OCT procedures. Informed consent was obtained from all patients, and the procedures adhered to the tenets of the Declaration of Helsinki. The study protocol was approved by the Institutional Review Committee of the Kyorin University School of Medicine, and all patients consented to our review of their medical records.

The surgery was performed by one of the three retina specialists (KH, MI, AH). After 2% lidocaine retrobulbar anesthesia, a standard three-port pars plana vitrectomy was performed to remove the ERM. Triamcinolone acetonide (MaQaid; Wakamoto Pharmaceutical Co., Ltd., Tokyo, Japan; or Kenacort-A; Bristol Pharmaceuticals KK, Tokyo, Japan) was injected intravitreally to make the vitreous gel and internal limiting membrane (ILM) more visible. This also allowed the surgeons to confirm that residual ERM and ILM were not present at the end of the vitrectomy.

Core vitrectomy was performed with the creation of a posterior vitreous detachment if it was not present; then the ERM and ILM were removed in all cases. The area of the ILM peeled was 2 to 3 optic disc diameters centered on the fovea. The lens was extracted from all patients > 55 years old, and all cataractous lenses were removed by phacoemulsification with an implantation of an intraocular lens. Anatomical success was defined as the complete removal of the ERM at the fovea as confirmed by slit-lamp biomicroscopy and SD-OCT. The main outcome measures were the postoperative BCVA and the condition of the foveal microstructures in the SD-OCT images at 12 months.

The patients had comprehensive ophthalmologic examinations before and 1, 3, 6, 9, and 12 months after the surgery. The examinations included measurements of the BCVA, binocular indirect ophthalmoscopy and noncontact lens slit-lamp biomicroscopy, and fundus photography. Spectral-domain–optical coherence tomography examinations were performed on all patients on the same day as the clinical examinations. The fovea was scanned, and the sections through the fovea were confirmed by the presence of the foveal bulge in the SD-OCT images. When a foveal bulge could not be identified, other morphological characteristics of the fovea, including a foveal depression, thinning of inner retinal layer in the SD-OCT images, and foveal avascular zone in the fundus images, were used as landmarks. The length of the COST line defect, IS/OS line defect, ELM line defect, and CFT were measured on the SD-OCT images.

A SD-OCT (OCT4000, Cirrus HD-OCT; Carl Zeiss Meditec, Inc., Dublin, CA) was used to record and analyze the images of the macular area. The entire macular area was scanned, and high-quality 6-mm scan images were obtained with the 5-line raster mode or high-definition 5-line raster mode. The length of the COST line defect, IS/OS line defect, and ELM line defect was measured with the software embedded in the SD-OCT system, and the lengths of the vertical and horizontal defects at the fovea were averaged. The CFT was defined as the maximum distance from the vitreoretinal surface to the RPE at the fovea. Two experienced investigators (YI, TR), who were masked to the patients' information including the postoperative period and the BCVA, measured each of the parameters on each SD-OCT image independently, and the average of the two investigators was used for the statistical analyses. Scans with a signal strength greater than 8/10 were examined, and a high-quality representative image was selected for the measurements. The axial length of the eye was measured with the Tomey OA1000 (Tomey Corp., Nagoya, Japan) preoperatively.

The decimal BCVA was converted to logarithm of minimal angle of resolution (logMAR) units for the statistical analyses. To compare two groups, Student's *t*-tests were used with continuous data. Multivariable analysis was also used to investigate the relationships between the BCVA and the preoperative or postoperative lengths of the COST line, IS/OS line, and ELM line defects at 1, 3, and 6 months. Simple linear regression analysis was used to determine the significance of correlations between the postoperative BCVA and preoperative or postoperative length of COST line defect. Forward stepwise regression analyses were performed to determine whether age, sex, symptom duration, axial length, CFT, and preoperative BCVA were significantly correlated with the BCVA at 12 months after the surgery.

Results

The preoperative baseline demographics of the 46 eyes are summarized in Table 1. The mean age of the patients was 67.4 ± 7.5 years with a range of 48 to 84 years. The mean preoperative decimal BCVA was 0.62 (Snellen equivalent, 20/30; 0.28 logMAR units). The mean postoperative follow-up period was 11.8 months with a range from 6 to 19 months. The interval between the onset of visual symptoms and the ERM surgery ranged from 1 to 70 months with a mean of 15.9 months. The mean axial length of the 41 phakic eyes was 23.8 mm with a range from 21.2 to 26.4 mm. A posterior vitreous

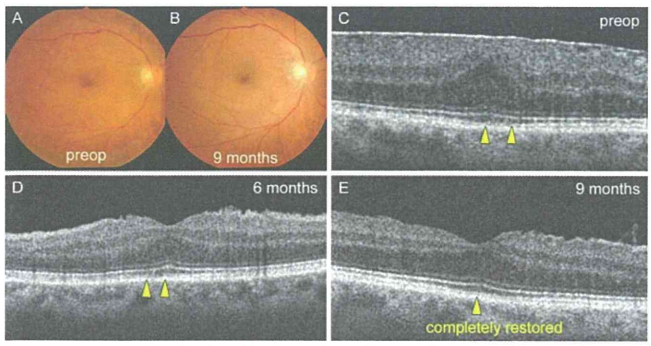

FIGURE 1. Fundus photographs and SD-OCT images of eyes after fully recovered COST line. (**A**) Preoperative fundus photograph showing an epiretinal membrane. The decimal BCVA was 0.6. (**B**) Postoperative fundus photograph at 9 months showing an absence of the epiretinal membrane. The BCVA has improved to 1.2. (**C**) Preoperative SD-OCT image of a horizontal scan showing a COST line defect with a length of 272 μm (*arrowheads*). (**D**) COST line defect is shorter at 6 months, to a length of 200 μm (*arrowheads*). (**E**) COST line is completely restored at 9 months (*arrowhead*).

detachment was not present in 9 eyes of 9 patients. None of the eyes had a recurrence of an ERM during the follow-up period.

The mean postoperative decimal BCVA was 0.81 (0.11 logMAR units) at 1 month, 0.93 (0.048 logMAR units) at 3 months, 0.96 (0.031 logMAR units) at 6 months, 1.0 (0.012 logMAR units) at 9 months, and 0.99 (0.016 logMAR units) at 12 months. Each postoperative BCVA was significantly better than the preoperative BCVA ($P < 0.0001$, Student's *t*-tests). The mean preoperative CFT was 463.0 ± 132.6 μm.

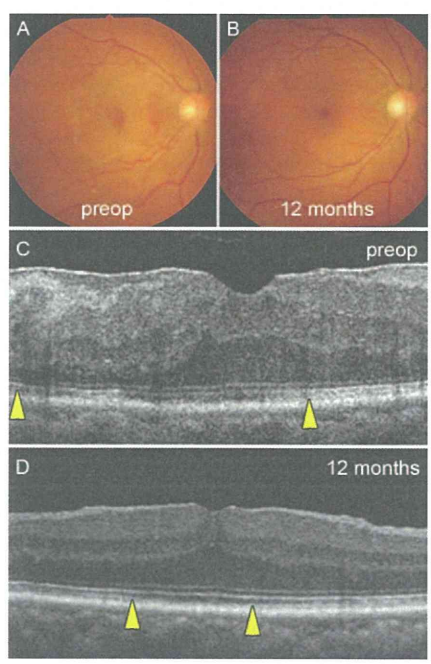

FIGURE 2. Fundus photographs and SD-OCT images of eyes with partially recovered COST line. (**A**) Preoperative fundus photograph showing an epiretinal membrane. The decimal BCVA was 0.3. (**B**) Postoperative fundus photograph at 12 months showing an absence of the epiretinal membrane. The BCVA has improved to 0.6. (**C**) Preoperative SD-OCT image of a vertical scan showing a COST line defect with a length of 2144 μm (*arrowheads*). (**D**) COST line defect remained at 12 months with a length of 936 μm (*arrowheads*).

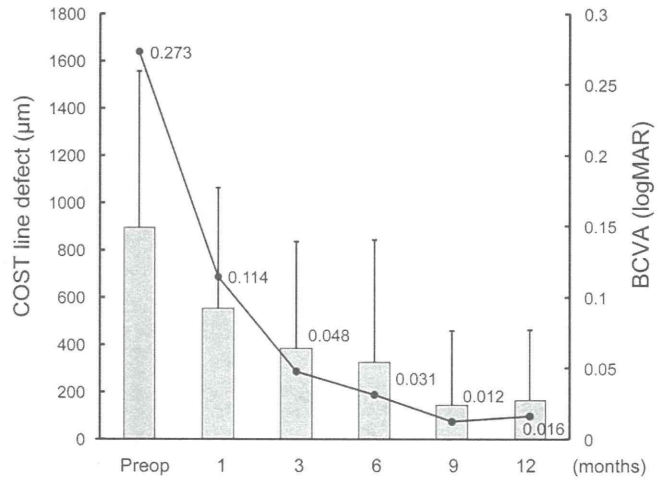

FIGURE 3. Correlation between the BCVA (*line plot*) and the mean length of the COST line defect (*bar chart*). The mean length of the COST line defect gradually decreases after surgery. The postoperative improvement of BCVA is significantly correlated with the decrease of the length of COST line defect.

Spectral-Domain–OCT of Foveal Microstructures

The preoperative mean length of the COST line defect was 893 ± 661 μm (mean ± standard deviation). The postoperative mean length of the COST line defect became gradually shorter, and the recovery began at the peripheral region and advanced toward the center of the macula (Figs. 1, 2). The mean length of COST line defect was 550 ± 511 μm at 1 month, 382 ± 450 μm at 3 months, 326 ± 517 μm at 6 months, 145 ± 344 μm at 9 months, and 165 ± 298 μm at 12 months (Fig. 3). The mean length of the COST line defect at each time was significantly shorter than the preoperative mean length ($P < 0.0001$, Student's *t*-tests). The postoperative decrease in the length of the COST line defect from the baseline was significantly correlated with improvement of the postoperative BCVA at 1 month ($r = 0.75$, $P < 0.01$; simple linear regression analysis), 3 months ($r = 0.70$, $P < 0.01$), 6 months ($r = 0.67$, $P < 0.01$), 9 months ($r = 0.68$, $P < 0.01$), and 12 months ($r = 0.61$, $P < 0.01$).

Forty-one eyes were examined 1 month after the surgery, and a well-restored IS/OS line and ELM line were detected in 35 eyes (85%), irregular IS/OS line but well-restored ELM line in 4 eyes (10%), and irregular IS/OS line and ELM line in 2 eyes (5%). The number of eyes with well-restored IS/OS and ELM lines gradually increased and that of irregular IS/OS line and ELM line gradually decreased during the postoperative period. At postoperative 9 months, the IS/OS and ELM lines were well restored in all 27 eyes. An intact COST line appeared only in eyes with a complete restoration of both the IS/OS and ELM lines, and the length of the COST line defect was usually longer than those of the IS/OS and ELM lines.

Correlation Between BCVA and Length of COST Line Defect

The correlation between the pre- or postoperative BCVA and the length of the COST line defect at each time point was determined by simple linear regression analysis.

The length of COST line defect was significantly correlated with the BCVA at each postoperative time ($P < 0.001$; Fig. 4).

Forward stepwise regression analysis was performed to determine whether the pre- and postoperative BCVAs were correlated with and affected by the postoperative length of the

Investigative Ophthalmology & Visual Science

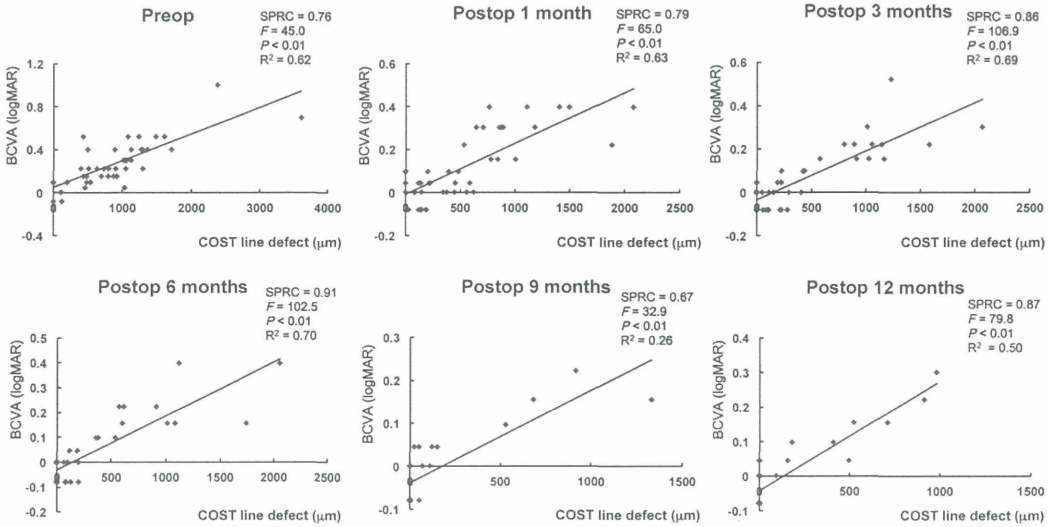

FIGURE 4. Correlation between length of the COST line defect and BCVA at each postoperative time determined by simple linear regression analysis. There are significant correlations between the length of the COST line defect and BCVA in the preoperative period and each postoperative period ($P < 0.01$). Preop, preoperative; Postop, postoperative; SPRC, standardized partial regression coefficients, $F = F$ value, $P = P$ value.

COST line, IS/OS line, or ELM line defects as causative factors. Our analyses showed that the BCVA was significantly correlated with the length of COST line defect preoperatively and at 1, 3, and 6 months postoperatively (R^2 value = 0.70, 0.65, 0.73, 0.71, respectively, $P < 0.001$ for all times; Table 2). After 9 months, the IS/OS and ELM lines were completely recovered in all cases, and we did not perform the multivariate statistical analysis.

The correlations between the postoperative BCVA and the preoperative length of the COST line defect, IS/OS line defect, and ELM line defect were also calculated. Forward stepwise regression analysis showed that the preoperative length of the COST line defect was significantly correlated with postoperative BCVA at 3, 6, 9, and 12 months ($P = 0.018$, 0.0005, 0.0005, 0.005, respectively), but not at 1 month ($P = 0.055$). The preoperative lengths of IS/OS line ($P = 0.76$, 0.89, 0.49, 0.09, 0.22, respectively) and ELM line defects ($P = 0.43$, 0.69, 0.16, 0.73, 0.89, respectively) were not significantly correlated with the BCVA at postoperative 1, 3, 6, 9, and 12 months.

Because the preoperative COST line defect was significantly correlated with the postoperative BCVA at 3, 6, 9, and 12 months by forward stepwise regression analysis, the correlation of the postoperative BCVA to the length of the COST line defect was evaluated at each time point by simple linear regression analysis. Our analyses showed that the preoperative length of the COST line defect was significantly correlated with the postoperative BCVA at postoperative 1, 3, 6, 9, and 12 months ($P = 0.047$ at postoperative 1 month, $P < 0.001$ at postoperative 3, 6, 9, and 12 months; Fig. 5). The relationship between the preoperative length of the COST line defect and the postoperative BCVA at 12 months is given by the following equation:

$$\text{BCVA} = 0.00010 \times L - 0.074$$

where the BCVA is the postoperative BCVA in logMAR units at 12 months and L is the preoperative length of the COST line defect in micrometers (95% confidence interval, 0.00006–0.00014). The estimation of the postoperative BCVA at 12 months from the preoperative length of COST line defect was significant (F value = 25.9, $R^2 = 0.40$; $P < 0.001$).

Relationship Between Patients' Demographics and Postoperative BCVA

The prognostic factors associated with the BCVA at 12 months postoperatively were determined by forward stepwise regression analysis (Table 3). The only preoperative factor that was significantly associated with the postoperative BCVA at 12 months was the preoperative length of the COST line defect (F value = 4.65, $P = 0.04$). Age, sex, axial length, presence of a posterior vitreous detachment (PVD), area of ILM peeling, symptom duration, use of triamcinolone acetonide, preoperative BCVA, and preoperative CFT were not significantly associated with the postoperative BCVA at 12 months (Table 3).

DISCUSSION

Four hyperreflective outer retinal bands have been identified in images obtained by SD-OCT. The innermost (first) line is the ELM line, which consists of the zonular adherences between the photoreceptor inner segments and the Müller cell processes.[26] The second hyperreflective band posterior to

TABLE 2. Forward Stepwise Regression Analysis Between SD-OCT Images and BCVA at 1, 3, and 6 Months Postoperatively

	Before Operation			1 Month			3 Months			6 Months		
	SPRC	*F* Value	*P* Value	SPRC	*F* Value	*P* Value	SPRC	*F* Value	*P* Value	SPRC	*F* Value	*P* Value
COST line defect	0.83	23.7	<0.001	0.77	43.9	<0.001	0.97	105.4	<0.001	0.9	60.8	<0.001
IS/OS line defect	0.41	2.10	0.15	−0.06	0.28	0.60	0.69	0.34	0.56	−0.57	0.72	0.40
ELM line defect	−0.53	4.2	0.09	0.15	2.21	0.14	−0.9	0.58	0.45	0.56	0.67	0.42

SPRC, standardized partial regression coefficients.

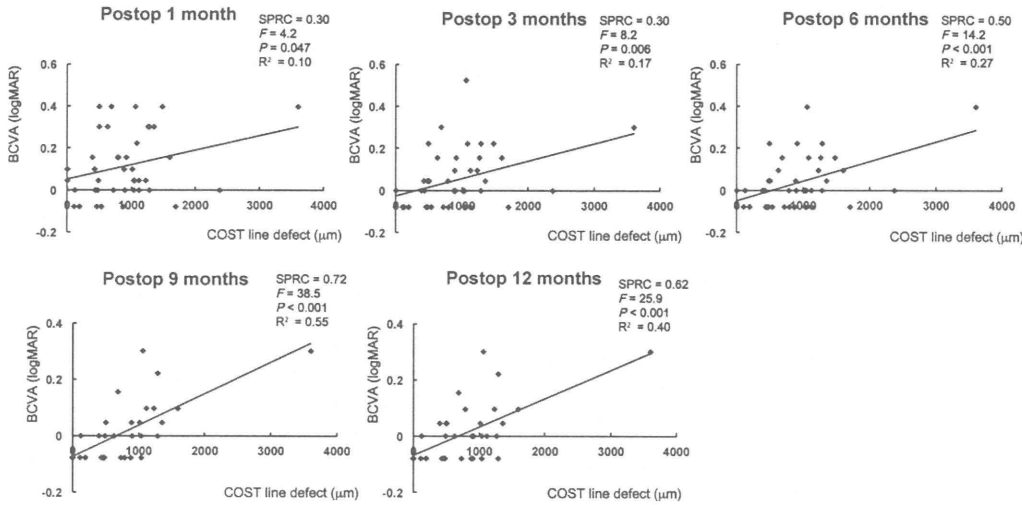

FIGURE 5. Correlation between preoperative length of COST line defect and postoperative BCVA by simple linear regression analysis. There are significant correlations between preoperative length of the COST line defect and BCVA at postoperative 1, 3, 6, 9, and 12 months.

the ELM line corresponds to the photoreceptor IS/OS line; and the third hyperreflective band posterior to the IS/OS line is the COST line, which is attributed to the scattering signals from the interface of the interdigitations between cone outer segments and the RPE microvillae.[26] The cone outer segments are shorter than the rod outer segments, and the RPE cell processes extend into the cone outer segment layer.[26] The fourth and deepest line represents the RPE layer.

Spaide and Curcio[27] demonstrated that the second band is aligned with the ellipsoid portion of the inner segments, and the third band corresponded to the ensheathment of the cone outer segments by the apical processes of the RPE in a structure known as the contact cylinder. These microstructures are vulnerable to various macular pathologies and can thus serve as hallmarks for the integrity of the photoreceptors.

Because the foveal microstructures were clearly observed in the SD-OCT images, we were able to measure the degree of integrity of the SD-OCT signals and calculate the correlation between the integrity of the photoreceptor microstructures and the postoperative BCVA. A reconstruction of the foveal ELM line in the early postoperative period is essential for the restoration of the foveal photoreceptor layer after macular hole surgery.[28]

The integrity of the photoreceptor IS/OS line has been extensively studied, and it has been reported that an intact IS/OS line was significantly associated with better postoperative BCVA after successful removal of an ERM.[5,11,14–16] Shimozono and associates[29] reported that the diameter of the IS/OS line and the COST line defects at 1 month was significantly correlated with the BCVA at 6 months but the COST line defect at baseline was not. The incidence of the eyes with disrupted COST line or IS/OS line at postoperative 1 month increased compared with base line, but then decreased after 6 months. The early postoperative status of the COST line was critical for later recovery of the BCVA; however, it included the effects of surgical invasion and postoperative inflammation.[29] Thus, the early postoperative status may not be a good predictive factor.

Our results indicated that there was a continuous postoperative recovery from 1 to 12 months, and forward stepwise regression analysis showed that the preoperative length of the COST line defect was significantly correlated with the postoperative BCVA from 3 to 12 months. Simple linear regression analysis showed a significant correlation from 1 to 12 months.

Shimozono and associates[29] stated that the reason the preoperative BCVA was not significantly correlated with the postoperative BCVA at 6 months was that they did not exclude patients with moderate cataracts. Our study included patients who had undergone combined cataract surgery with vitrectomy, and the postoperative recovery of BCVA may have been influenced by the status of the cataract in the patients with combined cataract surgery (phacovitrectomy), although eyes with severe cataract were not included in the study. Because the BCVA at baseline may be affected by the status of the lens, it is reasonable that the status of the COST line was the most important predictive factor for the postoperative BCVA irrespective of lens status. The COST line at baseline was also strongly correlated with the BCVA at baseline, which may indicate that the status of the lens did not strongly affect the BCVA at baseline.

Our study demonstrated that the preoperative length of the COST line defect was significantly correlated with the postoperative BCVA at 12 months, but that the preoperative lengths of the IS/OS line defect and the ELM line defect were not. We recently reported that the length of the COST line defect was significantly correlated with BCVA at each postoperative period from 3 to 12 months after macular hole surgery.[25] However, the lengths of IS/OS line defect and the ELM line defect were not significantly correlated with the BCVA 6 months after macular hole surgery.[25] These findings indicate that the recovery of the COST line was more

TABLE 3. Forward Stepwise Regression Analysis Between Patient Baseline Characteristics and BCVA at 12 Months Postoperatively

	SPRC	*F* Value	*P* Value
Age	−0.08	0.10	0.75
Sex	−0.19	0.56	0.46
Axial length	−0.14	0.29	0.59
Presence of PVD	0.23	0.50	0.48
ILM peeling	0.11	0.23	0.63
Types of adjuvant	−0.16	0.48	0.49
Symptom duration, mo	0.01	0.001	0.98
Preoperative BCVA	−0.16	0.17	0.69
COST line defect	0.74	4.65	0.04
CFT	−0.30	0.31	0.25

important for the postoperative BCVA than that of the IS/OS line and the ELM line after macular hole and ERM surgery.

The mean preoperative BCVA of our patients was 20/30, which was better than that of the average ERM candidate with BCVA more typically between 20/50 and 20/80. The recovery of the foveal COST line after successful macular hole surgery was correlated more strongly with eyes with postoperative BCVA better than 20/25. This may explain the stronger correlation between the BCVA and the COST line than with the IS/OS and ELM lines in our patients.[24]

The metamorphopsia caused by an ERM has been suggested to be due to a displacement of photoreceptors induced by tangential traction by the ERM on the retina.[30,31] In a physiological analysis by binocular correspondence perimetry, the metamorphopsia was found to be due to photoreceptor displacements in eyes with an ERM.[32] The COST line is located closer to the RPE layer than the IS/OS line, and the COST line signals may be reduced by the photoreceptor displacement because of a tilting of the photoreceptor outer segments. Adaptive optics scanning laser ophthalmoscopy images of eyes with an ERM showed an abnormal cone mosaic pattern similar to microfolds of the foveal photoreceptor layer.[33] The location of the abnormal cone mosaic pattern corresponded to the sites of IS/OS line disruption.[33] The COST line may be disrupted by a similar mechanism. Decreased cone densities with altered cone mosaic patterns were detected by adaptive optics scanning laser ophthalmoscopy in eyes with a disrupted IS/OS line or COST line in patients with central serous chorioretinopathy.[21] Poor interdigitation of cone photoreceptor cells and the underlying RPE can result in a disruption of the COST line.

The CFT has been reported to be significantly correlated with the BCVA and to be a prognostic factor for the postoperative BCVA after ERM removal.[1,3] Our results showed that the preoperative CFT was not significantly correlated with the postoperative BCVA as previously reported.[5,11,15,34] Although these opposing results may be due to different study populations and different methods of evaluation, the CFT does not appear to be a major prognostic factor compared with the integrity of the COST line. We did not evaluate the presence of a dissociated optic nerve fiber layer (DONFL) appearance, which is frequently found in eyes after vitrectomy with ILM peeling for ERM of macular hole. However, the presence of DONFL has been reported to not preclude postoperative good visual recovery.[35] We also did not use microperimetry to evaluate the retinal sensitivity in the area of the COST line defect. This is relevant because it has been reported that the preoperative lengths of the IS/OS and ELM line defect were associated with the foveal sensitivity at 6 months after surgery in macular hole patients.[36]

There are limitations to this study. This was a retrospective study without a control group. Also, the number of patients in each group was small, and the resolution of SD-OCT used may not have been sufficient to detect the COST line compared to high-speed ultrahigh-resolution OCT. Furthermore, even with the higher spatial resolution SD-OCT instruments, the foveal center can be missed, which results in lower-intensity images and evaluation of the wrong area of the fovea. Therefore, further studies with a larger sample size and higher-resolution SD-OCT are needed to confirm the results of this study.

In summary, our quantitative measurements of the photoreceptor COST line defects showed that the recovery of photoreceptor COST line was correlated with the postoperative BCVA after ERM surgery. We also found that the preoperative length of the COST line defect may predict the postoperative BCVA after successful ERM removal and the potential foveal function.

Acknowledgments

Disclosure: **Y. Itoh**, None; **M. Inoue**, None; **T. Rii**, None; **K. Hirota**, None; **A. Hirakata**, None

References

1. Wilkins JR, Puliafito CA, Hee MR, et al. Characterization of epiretinal membranes using optical coherence tomography. *Ophthalmology*. 1996;103:2142–2151.
2. Michalewski J, Michalewska Z, Cisiecki S, Nawrocki J. Morphologically functional correlations of macular pathology connected with epiretinal membrane formation in spectral optical coherence tomography (SOCT). *Graefes Arch Clin Exp Ophthalmol*. 2007;245:1623–1631.
3. Suh MH, Seo JM, Park KH, Yu HG. Associations between macular findings by optical coherence tomography and visual outcomes after epiretinal membrane removal. *Am J Ophthalmol*. 2009;147:473–480.
4. Tsunoda K, Watanabe K, Akiyama K, Usui T, Noda T. Highly reflective foveal region in optical coherence tomography in eyes with vitreomacular traction or epiretinal membrane. *Ophthalmology*. 2012;119:581–587.
5. Inoue M, Morita S, Watanabe Y, et al. Preoperative inner segment/outer segment junction in spectral-domain optical coherence tomography as a prognostic factor in epiretinal membrane surgery. *Retina*. 2011;31:1366–1372.
6. Machemer R. The surgical removal of epiretinal macular membranes (macular puckers) [in German]. *Klin Monbl Augenheilkd*. 1978;173:36–42.
7. Wolf S, Wolf-Schnurrbusch U. Spectral-domain optical coherence tomography use in macular diseases: a review. *Ophthalmologica*. 2010;224:333–340.
8. Koizumi H, Spaide RF, Fisher YL, et al. Three-dimensional evaluation of vitreomacular traction and epiretinal membrane using spectral-domain optical coherence tomography. *Am J Ophthalmol*. 2008;145:509–517.
9. Chang LK, Fine HF, Spaide RF, Koizumi H, Grossniklaus HE. Ultrastructural correlation of spectral-domain optical coherence tomographic findings in vitreomacular traction syndrome. *Am J Ophthalmol*. 2008;146:121–127.
10. Gaudric A. Macular cysts, holes and cavitations: 2006 Jules Gonin lecture of the Retina Research Foundation. *Graefes Arch Clin Exp Ophthalmol*. 2008;246:1071–1079.
11. Falkner-Radler CI, Glittenberg C, Hagen S, Benesch T, Binder S. Spectral-domain optical coherence tomography for monitoring epiretinal membrane surgery. *Ophthalmology*. 2010;117:798–805.
12. Takahashi A, Nagaoka T, Ishiko S, Kameyama D, Yoshida A. Foveal anatomic changes in a progressing stage 1 macular hole documented by spectral-domain optical coherence tomography. *Ophthalmology*. 2010;117:806–810.
13. Odrobina D, Michalewska Z, Michalewski J, Dzięgielewski K, Nawrocki J. Long-term evaluation of vitreomacular traction disorder in spectral-domain optical coherence tomography. *Retina*. 2011;31:324–331.
14. Kim JH, Kim YM, Chung EJ, Lee SY, Koh HJ. Structural and functional predictors of visual outcome of epiretinal membrane surgery. *Am J Ophthalmol*. 2012;153:103–110.
15. Mitamura Y, Hirano K, Baba T, Yamamoto S. Correlation of visual recovery with presence of photoreceptor inner/outer segment junction in optical coherence images after epiretinal membrane surgery. *Br J Ophthalmol*. 2009;93:171–175.
16. Inoue M, Morita S, Watanabe Y, et al. Inner segment/outer segment junction assessed by spectral-domain optical coherence tomography in patients with idiopathic epiretinal membrane. *Am J Ophthalmol*. 2010;150:834–839.

Investigative Ophthalmology & Visual Science

17. Srinivasan VJ, Monson BK, Wojtkowski M, et al. Characterization of outer retinal morphology with high-speed, ultrahigh-resolution optical coherence tomography. *Invest Ophthalmol Vis Sci*. 2008;49:1571–1579.
18. Rii T, Itoh Y, Inoue M, Hirakata A. Foveal cone outer segment tips line and disruption artifacts in spectral-domain optical coherence tomographic images of normal eyes. *Am J Ophthalmol*. 2012;153:524–529.
19. Park SJ, Woo SJ, Park KH, Hwang JM, Chung H. Morphologic photoreceptor abnormality in occult macular dystrophy on spectral-domain optical coherence tomography. *Invest Ophthalmol Vis Sci*. 2010;51:3673–3679.
20. Puche N, Querques G, Benhamou N, et al. High-resolution spectral domain optical coherence tomography features in adult onset foveomacular vitelliform dystrophy. *Br J Ophthalmol*. 2010;94:1190–1196.
21. Ooto S, Hangai M, Sakamoto A, et al. High-resolution imaging of resolved central serous chorioretinopathy using adaptive optics scanning laser ophthalmoscopy. *Ophthalmology*. 2010; 117:1800–1809.
22. Lai WW, Leung GY, Chan CW, Yeung IY, Wong D. Simultaneous spectral domain OCT and fundus autofluorescence imaging of the macula and microperimetric correspondence after successful repair of rhegmatogenous retinal detachment. *Br J Ophthalmol*. 2010;94:311–318.
23. Cheung CM, Yeo IY, Koh A. Photoreceptor changes in acute and resolved acute posterior multifocal placoid pigment epitheliopathy documented by spectral-domain optical coherence tomography. *Arch Ophthalmol*. 2010;128:644–646.
24. Itoh Y, Inoue M, Rii T, Hiraoka T, Hirakata A. Significant correlation between visual acuity and recovery of foveal cone microstructures after macular hole surgery. *Am J Ophthalmol*. 2012;153:111–119.
25. Itoh Y, Inoue M, Rii T, Hiraoka T, Hirakata A. Correlation between length of foveal cone outer segment tips line defect and visual acuity after macular hole closure. *Ophthalmology*. 2012;119:1438–1446.
26. Gloesmann M, Hermann B, Schubert C, et al. Histologic correlation of pig retina radial stratification with ultrahigh-resolution optical coherence tomography. *Invest Ophthalmol Vis Sci*. 2003;44:1696–1703.
27. Spaide RF, Curcio CA. Anatomical correlates to the bands seen in the outer retina by optical coherence tomography: literature review and model. *Retina*. 2011;31:1609–1619.
28. Wakabayashi T, Fujiwara M, Sakaguchi H, Kusaka S, Oshima Y. Foveal microstructure and visual acuity in surgically closed macular holes: spectral-domain optical coherence tomographic analysis. *Ophthalmology*. 2010;117:1815–1824.
29. Shimozono M, Oishi A, Hata M, et al. The significance of cone outer segment tips as a prognostic factor in epiretinal membrane surgery. *Am J Ophthalmol*. 2012;153:698–704.
30. Michels RG. A clinical and histopathologic study of epiretinal membranes affecting the macula and removed by vitreous surgery. *Trans Am Ophthalmol Soc*. 1982;80:580–656.
31. McDonald HR, Johnson RN, Ai E, et al. Macular epiretinal membranes. In: Ryan SJ, Schachat AP, Wilkinson CP, et al., eds. *Retina*. 4th ed. Philadelphia: Elsevier/Mosby; 2005:2509–2525.
32. Krøyer K, Jensen OM, Larsen M. Objective signs of photoreceptor displacement by binocular correspondence perimetry: a study of epiretinal membranes. *Invest Ophthalmol Vis Sci*. 2005;46:1017–1022.
33. Ooto S, Hangai M, Takayama K, et al. High-resolution imaging of the photoreceptor layer in epiretinal membrane using adaptive optics scanning laser ophthalmoscopy. *Ophthalmology*. 2011;118:873–881.
34. Massin P, Allouch C, Haouchine B, et al. Optical coherence tomography of idiopathic macular epiretinal membranes before and after surgery. *Am J Ophthalmol*. 2000;130:732–739.
35. Tadayoni R, Paques M, Massin P, et al. Dissociated optic nerve fiber layer appearance of the fundus after idiopathic epiretinal membrane removal. *Ophthalmology*. 2001;108:2279–2283.
36. Ooka E, Mitamura Y, Baba T, et al. Foveal microstructure on spectral-domain optical coherence tomographic images and visual function after macular hole surgery. *Am J Ophthalmol*. 2011;152:283–290.

Investigative Ophthalmology & Visual Science

PAIN® 154 (2013) 1352–1357

PAIN®

www.elsevier.com/locate/pain

Cortical excitability changes after high-frequency repetitive transcranial magnetic stimulation for central poststroke pain

Koichi Hosomi [a,b], Haruhiko Kishima [b], Satoru Oshino [b], Masayuki Hirata [b], Naoki Tani [b,c], Tomoyuki Maruo [a,b], Shiro Yorifuji [d], Toshiki Yoshimine [b], Youichi Saitoh [a,b,*]

[a] Department of Neuromodulation and Neurosurgery, Office for University–Industry Collaboration, Osaka University, 2-1 Yamadaoka, Suita, Osaka 565-0871, Japan
[b] Department of Neurosurgery, Osaka University Graduate School of Medicine, 2-2 Yamadaoka, Suita, Osaka 565-0871, Japan
[c] Department of Neurosurgery, Otemae Hospital, 1-5-34 Otemae, Chuo-ku, Osaka 540-0008, Japan
[d] Department of Functional Diagnostic Science, Osaka University Graduate School of Medicine, 1-7 Yamadaoka, Suita, Osaka 565-0871, Japan

Sponsorships or competing interests that may be relevant to content are disclosed at the end of this article.

ARTICLE INFO

Article history:
Received 23 October 2012
Received in revised form 31 March 2013
Accepted 8 April 2013

Keywords:
Central poststroke pain
Cortical excitability
Intracortical facilitation
Motor cortex stimulation
Primary motor cortex
Repetitive transcranial magnetic stimulation

ABSTRACT

Central poststroke pain (CPSP) is one of the most refractory chronic pain syndromes. Repetitive transcranial magnetic stimulation (rTMS) of the primary motor cortex has been demonstrated to provide moderate pain relief for CPSP. However, the mechanism underlying the pain relief remains unclear. The objective of this study was to assess changes in cortical excitability in patients with intractable CPSP before and after rTMS of the primary motor cortex. Subjects were 21 patients with CPSP of the hand who underwent rTMS. The resting motor threshold, the amplitude of the motor evoked potential, duration of the cortical silent period, short interval intracortical inhibition, and intracortical facilitation were measured as parameters of cortical excitability before and after navigation-guided 5 Hz rTMS of the primary motor cortex corresponding to the painful hand. Pain reduction from rTMS was assessed with a visual analog scale. The same parameters were measured in both hemispheres of 8 healthy controls. Eight of 21 patients experienced $\geqslant$30% pain reduction after rTMS (responders). The resting motor threshold in the patients was higher than those in the controls at baseline ($P = .035$). Intracortical facilitation in the responders was lower than in the controls and the nonresponders at baseline ($P = .035$ and $P = .019$), and significantly increased after rTMS ($P = .039$). There were no significant differences or changes in the other parameters. Our findings suggest that restoration of abnormal cortical excitability might be one of the mechanisms underlying pain relief as a result of rTMS in CPSP.

1. Introduction

Central poststroke pain (CPSP) is one of the most refractory neuropathic pains caused by the brain lesion of the somatosensory nervous system after cerebrovascular accident, with a reported incidence of 1–8% among poststroke patients [1,3]. These pain symptoms almost always develop within the area of sensory disturbances and have been described as burning, numb, aching, squeezing, or pricking. Medical treatments for CPSP often fail to relieve the pain, and symptoms are persistent in approximately 85% of patients. These pain conditions often disturb poststroke rehabilitation and activities of daily life, thereby reducing the patient's quality of life [18].

For these refractory disease conditions, the electrical motor cortex stimulation (EMCS), whose common target is the precentral gyrus (primary motor cortex; M1), has provided relief in 26–73% of CPSP patients [15,16,33,36,42,43,46]. However, EMCS involves invasive surgery, which requires intracranial electrodes and an implantable pulse generator. In addition, several perioperative complications including stimulation-induced seizure, infection, epidural hematoma, and neurological deterioration have been reported [15,16,33,36,42,43,46]. According to recent reports, noninvasive repetitive transcranial magnetic stimulation (rTMS) can have positive effects in patients with intractable CPSP similar to that of EMCS [2,4,14,17,26,28,41]. Several meta-analyses and systematic reviews have demonstrated that the high-frequency ($\geqslant$5 Hz) rTMS of M1 provides modest and short-lasting effects on neuropathic pain, including CPSP [30,32,34].

The mechanisms underlying rTMS effects on CPSP remain to be elucidated. It has been suggested in several previous reports that EMCS and rTMS of M1 affect the local stimulus sites in M1 and

* Corresponding author at: Department of Neuromodulation and Neurosurgery, Office for University–Industry Collaboration, Osaka University, 2-1 Yamadaoka, Suita, Osaka 565-0871, Japan. Tel./fax: +81 6 6879 4138.
E-mail address: neurosaitoh@mbk.nifty.com (Y. Saitoh).

0304-3959/$36.00
http://dx.doi.org/10.1016/j.pain.2013.04.017

the various remote structures that are functionally associated with M1 and involved in chronic pain and pain relief [24,30]. Two positron emission tomography (PET) studies demonstrated that motor cortex stimulation increased the regional cerebral blood flow in the various structures related to pain perception and the emotional aspects of pain, such as the thalamus, insula, limbic system, and upper brain stem [11,19]. Lefaucheur et al. reported that rTMS of M1 restored defective intracortical inhibition in patients with chronic neuropathic pain and proved the alterations within the stimulus site [27]. However, the patient characteristics in these previous reports were heterogeneous. These subjects were patients with CPSP, but some also had neuropathic pain due to spinal or peripheral nerve lesions.

In this study, we concentrated the rTMS effects within M1 in patients with CPSP. A single- or paired-pulse transcranial magnetic stimulation (TMS) allowed us to evaluate the cortical excitability of M1, measuring motor evoked potentials (MEP) [23,47]. The objective of this study was to assess the alterations of cortical excitability in patients with intractable CPSP before and after rTMS of M1.

2. Methods

2.1. Subjects

Subjects were 21 consecutive patients with CPSP (12 men and 9 women), with a mean ± standard deviation age of 59.6 ± 9.0 years and with an average pain duration of 48.1 ± 55.0 months before the experiment. All patients were diagnosed with CPSP according to the following criteria [20]: (1) development of pain after stroke, (2) sensory disturbance corresponding to the cerebral lesion, (3) pain located within the region of sensory disturbance, and (4) exclusion of other causes of pain. All patients had an intractable continuous pain in their hand lasting more than 6 months despite appropriate medical treatments. We excluded patients with severe motor weakness corresponding to less than grade 2 in the manual muscle test because of the insufficient MEP evoked by TMS in the affected hand. The lesions from stroke were located in the thalamus ($n = 8$), putamen ($n = 7$), brain stem ($n = 4$), and subcortex ($n = 2$). All the patients had a sensory deficit in their painful zone and described their pain as burning, aching, squeezing, pricking, or numb; pain occurred in the unilateral body including the hand. Allodynia was observed in 13 patients (62%) and hyperpathia in 4 patients (19%). Patient characteristics and clinical data are summarized in Table 1.

Eight healthy volunteers were also enrolled onto this study (8 men; mean age, 52.5 ± 10.0 years). All subjects were right-handed. They had no neurological diseases, and no lesions were evident on magnetic resonance imaging.

2.2. Overview of experiments

A session of 5 Hz rTMS of M1 corresponding to the painful hand was applied to all the patients [14,41]. Cortical excitability within M1 was evaluated by the single- or paired-pulse TMS before and after an rTMS session. Cortical excitability was measured in the same side as rTMS performance. Pain intensity was examined in each patient before and after rTMS using a visual analog scale (VAS). The healthy controls underwent the same single- or paired-pulse TMS measurements in M1 of both hemispheres. We assessed alterations in cortical excitability and the relationship between pain relief and cortical excitability changes.

The ethics committee of Osaka University Hospital approved this study (approval 07099), and written informed consent was obtained from all subjects participating in this study.

2.3. Motor cortical excitability testing

Motor cortical excitability testing was applied by the single- or paired-pulse TMS using a reversed-current, figure-8 double 70-mm coil (Magstim Company, Carmarthenshire, UK) and the Magstim 200 magnetic stimulator (Magstim Company). A Magstim 200 magnetic stimulator provides single monophasic pulses. Two Magstim 200 magnetic stimulators were connected to a Bistim module (Magstim Company) delivering paired pulses. Subjects lay down on the bed to keep their hands relaxed, and their heads were fixed to avoid displacement of the stimulus site during cortical excitability testing and rTMS. The center of the TMS coil was placed on M1 corresponding to the hand using the optical TMS navigation system (Brainsight, Rogue Research Inc, Montreal, Quebec, Canada) and fixed by means of an articulated coil holder. The handle of the reversed-current coil was directed anteromedially so that the intracerebral current was induced to the same direction as the standard double coil handle placed in the posterolateral direction. Finally, the optimal stimulus site was determined on the basis of the highest amplitude MEP in the abductor pollicis brevis (APB) muscles. The MEPs were recorded from surface electrodes placed on the belly and tendon of the contralateral APB muscles through a 20 to 3000 Hz band-pass filter using Neuropack electromyography (MEB-2208, Nihon Kohden, Tokyo, Japan).

Five indices, including (1) resting motor threshold (RMT), (2) MEP amplitude at 120% of RMT (MEP120), (3) cortical silent period (CSP), (4) short interval intracortical inhibition (SICI), and (5) intracortical facilitation (ICF), were measured as parameters of motor cortical excitability. The RMT was defined as the minimum stimulus intensity evoking MEPs of $\geqslant 50$ μV at least 5 of 10 times under complete muscle relaxation [39]. RMT was measured by reducing the stimulus intensity in steps of 1% from the suprathreshold intensity. Complete muscle relaxation was monitored by the electromyograms (EMG) from the APB muscles. Subsequently, 15 MEPs were recorded at 120% of RMT, and the average peak-to-peak amplitude of MEPs was determined as MEP120. CSP was measured by single TMS pulses at 130% of RMT, while subjects executed a continuous maximum voluntary contraction of their APB muscles. To ensure adequate contractions of the target muscle, EMG feedback was provided for the subjects. Eight trials were rectified and superimposed. CSP was defined as the minimum duration from stimulus delivery to the return of voluntary activity [21]. Paired-pulse stimulation was performed in accordance with Kujirai et al. [23]. A conditioning stimulus was set at 80% of RMT, and a test stimulus was set at 120% of RMT. Interstimulus intervals were set at 2 and 4 ms for SICI, and 10 and 15 ms for ICF. Ten trials of each interstimulus interval were randomly intermixed with nonconditioned trials (test stimulus only). Finally, a total of 50 trials were delivered, and the average peak-to-peak MEP amplitude ($MEP_{conditioned}$) was calculated for each condition. SICI and ICF were defined follows: $SICI = 100\% - (MEP_{conditioned}/MEP_{nonconditioned})$ and $ICF = MEP_{conditioned}/MEP_{nonconditioned}$. Each stimulation was separated by at least 5 s in order to avoid carryover effects.

2.4. rTMS procedure

The rTMS was applied through a figure-8 coil (MC B-70, Medtronic Functional Diagnostics A/S, Skovlunde, Denmark) and connected to a MagPro magnetic stimulator (Medtronic Functional Diagnostics A/S), which provides repetitive biphasic pulses. The TMS coil was placed with the optical TMS navigation system (Brainsight) and fixed by the coil holder in the same way used for motor cortical excitability testing. The RMT was determined by stimulation of the region of M1 corresponding to the hand representation. A potential equivalent to 90% intensity of RMT was used for repetitive stimulation. Ten trains of 5 Hz rTMS were delivered